Journal of
Composites Science

MDPI

Article

Enhancing Polycaprolactone with Levulinic Acid-Extracted Lignin: Toward Sustainable Bio-Based Polymer Blends

Elodie Melro [1,2,*], Hugo Duarte [3,4,*], Filipe E. Antunes [1,2], Artur J. M. Valente [2], Anabela Romano [4] and Bruno Medronho [4,5,*]

1 Science 351, Instituto Pedro Nunes, Rua Pedro Nunes, 3030-199 Coimbra, Portugal; filipe.antunes@science351.pt
2 CQC-IMS, Department of Chemistry, University of Coimbra, Rua Larga, 3004-535 Coimbra, Portugal; avalente@ci.uc.pt
3 Chemical Engineering and Renewable Resources for Sustainability (CERES), Department of Chemical Engineering, University of Coimbra, Rua Sílvio Lima, Pólo II, Pinhal de Marrocos, 3030-790 Coimbra, Portugal
4 MED–Mediterranean Institute for Agriculture, Environment and Development, CHANGE–Global Change and Sustainability Institute, Faculdade de Ciências e Tecnologia, Universidade do Algarve, Campus de Gambelas, Ed. 8, 8005-139 Faro, Portugal; aromano@ualg.pt
5 FSCN, Surface and Colloid Engineering, Mid Sweden University, SE-851 70 Sundsvall, Sweden
* Correspondence: elodie.melro@science351.pt (E.M.); uc49007@uc.pt (H.D.); bfmedronho@ualg.pt (B.M.)

Abstract

The growing demand for sustainable materials has intensified the search for biodegradable polymers. Poly(ε-caprolactone) (PCL), though biodegradable, is fossil-derived. In this study, a novel lignin extracted from pine wood using a green solvent was incorporated into PCL and compared with commercial lignins (dealkaline, alkaline, and lignosulfonate). The lignin additions imparted antioxidant properties, enhanced thermal stability, and promoted circular economy goals through lignin valorization. Notably, the green-extracted lignin showed superior compatibility with PCL when compared with commercial lignins, as evidenced by lower water uptake and solubility, and improved surface hydrophobicity (higher contact angle). Although the addition of lignin reduced the tensile strength and elongation at break, it greatly increased the PCL radical scavenging activity (DPPH) from 8 ± 1% of neat PCL to 94.8 ± 0.3% when 20 wt% of lignin-LA was added. Among the tested lignins, lignin-LA stands out as the most promising candidate to be applied as a functional additive in biodegradable polymer blends and composites for advanced sustainable applications. Not only given its intrinsically higher sustainability but also due to its capacity for improving the thermal properties of PCL–lignin blends.

Keywords: biodegradable polymers; Poly(ε-caprolactone) (PCL); lignin; levulinic acid; sustainable materials

Received: 20 May 2025
Revised: 2 July 2025
Accepted: 4 July 2025
Published: 14 July 2025

Citation: Melro, E.; Duarte, H.; Antunes, F.E.; Valente, A.J.M.; Romano, A.; Medronho, B. Enhancing Polycaprolactone with Levulinic Acid-Extracted Lignin: Toward Sustainable Bio-Based Polymer Blends. *J. Compos. Sci.* **2025**, *9*, 366. https://doi.org/10.3390/jcs9070366

1. Introduction

Poly(ε-caprolactone) (PCL) is a semicrystalline, biodegradable aliphatic polyester that is synthesized either via the condensation of 6-hydroxyhexanoic acid or, more commonly, through the ring-opening polymerization (ROP) of ε-caprolactone [1]. ROP is preferred due to its mild reaction conditions, absence of side reactions, and capability of producing polyesters with controlled molecular weights [2].

During the last few decades, several biodegradable polymers have been developed, with a special interest in PCL due to its favorable physicochemical properties and compatibility with other polymers. PCL exhibits excellent processability due to its low melting

point (55–60 °C), low glass transition temperature (−60 °C), and high thermal decomposition temperature (~350 °C) [3–5]. These features make PCL suitable for applications ranging from biomedical devices to sustainable packaging [6,7]. PCL degrades completely over a period of ca. 3 to 4 years, typically through a two-step mechanism: (1) an initial non-enzymatic hydrolytic cleavage of the ester bonds and (2) intracellular degradation when the PCL's molecular weight drops below 3000 Da and its crystallinity is high [8,9].

Another promising biopolymer is lignin, which is considered one of the most abundant natural polymers on Earth. Despite its promising functional properties, it remains largely underutilized [10]. Lignin is a complex, amorphous, and polyphenolic polymer composed of p-coumaryl, coniferyl, and sinapyl alcohol units, which are interconnected by several linkages such as β-O-4, β-β, and 5-5 bonds. It serves a structural role in plant cell walls and exhibits high carbon content, thermal stability, UV absorption, antioxidant activity, biodegradability, renewability, and low cost, making its use very attractive for several applications [11,12]. The performance of lignin in polymeric matrices depends on its origin and extraction method, which give rise to structurally distinct types. Kraft lignin, produced under alkaline conditions, contains sulfur and is highly condensed. Lignosulfonates, obtained from sulfite pulping, are water-soluble, organosolv lignin is sulfur-free and of high purity, and soda lignin has a high phenolic content and is derived from non-wood biomass [13]. These differences impact molecular weight, solubility, and reactivity in polymer systems [12]. Because of the complex and heterogeneous structure of lignin, as well as the limited availability of functional groups compatible with most polymer matrices, the chemical modification of lignin is often necessary, including processes such as acetylation, silanization, succinylation, and copolymerization via ring-opening reactions [14]. A promising approach involves grafting lactide or lactic acid into lignin to form lignin-g-PLA copolymers [15,16]. However, such strategies have been studied less and are more synthetically demanding in the case of PCL, due to its lower polarity and limited reactivity.

Lignin incorporation into PCL matrices is more commonly achieved via blends or composites, which can add value to industrial lignin waste while enhancing the final material performance. Blends and composites offer processing flexibility and allow for easier formulation compared to covalently bonded systems [17,18]. Previous studies on PCL/lignin systems have explored a range of lignin sources, such as kraft lignin, organosolv lignin esters, alcell lignin, and lignin from straw via steam explosion, often in combination with lignosulfonates [19–24]. In this work, for the first time, we evaluate the effect of several commercial lignins and a novel lignin extracted from pine wood using levulinic acid—a green solvent—on the preparation and properties of lignin/PCL blends. This unique comparative study aims to provide insights into the compatibility, performance, and sustainable potential of these novel bio-based composites.

2. Materials and Methods

2.1. Materials

PCL (6000 Da), dealkaline lignin, alkaline lignin, sodium lignosulfonate, and 2,2-diphenyl-1-picrylhydrazyl (≥97.0%) free radical were purchased from the Tokyo Chemical Industry (TCI). Methanol was obtained from José Manuel Gomes dos Santos, Lda. (Porto, Portugal), levulinic acid (98%) was purchased from Sigma-Aldrich, and hydrochloric acid (37%) was purchased from Fisher Scientific. Maritime pine (*Pinus pinaster* Ait.) sawdust was supplied by Valco—Madeiras e Derivados, S.A. (Leiria, Portugal).

2.2. Methods

2.2.1. Lignin Fractionation and Extraction from Pine Wood Sawdust Residues

A new sustainable levulinic acid-based solvent has been developed for the efficient fractionation and extraction of lignin from various lignocellulosic sources [25]. Briefly, the solvent consists of levulinic acid, with 0.1 M HCl used as a catalyst, and the optimized fractionation conditions were set at 140 °C for 2 h. A detailed characterization of the extracted lignin and its purification using levulinic acid-based systems has been previously described by some of us and can be found elsewhere [25,26].

2.2.2. PCL–Lignin Blends

Lignin/PCL blends were prepared by incorporating varying amounts of dealkaline lignin (0, 10, 20, 30, 40, 50, 60, 70, 80, 90, and 100 wt%) or different types of lignin at a fixed concentration (i.e., 20 wt%), with the lignin content calculated relative to the weight of the PCL. The mixing was performed using a two-roll mill blender (Thermo Scientific—Haake Polylab QC, Germany). Firstly, PCL was melted at 100 °C for 3 min at 60 rpm, and then lignin was added and continuously mixed until a constant torque was observed (ca. 10–15 min). During this period, the torque response was recorded.

2.2.3. Water Absorption

Water absorption testing was adapted from ASTM D570-98 [27]. Square samples (2 × 2 × 0.1 mm) were pre-dried in an oven at 50 °C for 24 h, cooled to room temperature in a desiccator, and weighed (W_0). Then, the samples were immersed in 50 mL of distilled water at room temperature. At predetermined intervals, samples were removed, gently blotted with a paper towel to remove excess superficial water, and weighed (W_1). All measurements were performed in triplicate. Water absorption (%) was calculated using the following formula:

$$\text{Water absorption}(\%) = \frac{W_1 - W_0}{W_0} \cdot 100 \quad (1)$$

The water sorption kinetics was first evaluated by using the power law equation, as follows [28]:

$$\frac{m_{w,t}}{m_{w,eq}} = kt^n \quad (2)$$

where, $m_{w,t}$ and $m_{w,eq}$ are the masses of the water sorbed by the blend at time t and at equilibrium, respectively, n is the exponent that describes the water diffusion mechanism, and k is the kinetic constant. Equation (2) is applied to cumulative water sorption up to 60%.

2.2.4. Water Solubility

All swollen samples from the water absorption tests were used to determine water solubility, following ASTM D570-98 [28]. The swollen specimens were dried in an oven at 60 °C for 24 h, cooled to room temperature in a desiccator, and weighed (W_2). Three samples of each composition were analyzed. Water solubility (%) was calculated using the following equation:

$$\text{Water solubility}(\%) = \frac{W_0 - W_2}{W_0} \cdot 100 \quad (3)$$

2.2.5. Contact Angle

Water contact angle measurements were performed using a contact angle meter (Attension Theta Flex, Biolin Scientific, Gothenburg, Sweden). The hot-pressed samples were mounted on the movable stage, and an 8 µL droplet of distilled water was carefully placed on the surface. Ten measurements were taken for each composite formulation.

2.2.6. Antioxidant Properties

The DPPH radical method was used to evaluate the antioxidant activity [29]. Samples (0.2 g) were cut into small pieces and immersed in 4 mL of methanol for 24 h at room temperature. After incubation, the mixture was centrifuged for 2 min at 3000 rpm to minimize potential interference from air bubbles, impurities, or transient aggregates in the UV-Vis absorbance measurements. An aliquot of 1.5 mL was mixed with 1.5 mL of a 50 mg.L^{-1} DPPH solution in methanol. The mixture was kept in the dark at room temperature for 60 min, and the absorbance was measured at 517 nm using a UV-Vis spectrophotometer (Shimadzu UV-2450, Shimadzu Corporation, Kyoto, Japan). The experiment was performed in triplicate, and the radical scavenging activity (RSA) was calculated as follows:

$$\mathrm{RSA}(\%) = \frac{\mathrm{A_{control}} - \mathrm{A_{sample}}}{\mathrm{A_{control}}} \cdot 100 \quad (4)$$

2.2.7. Fourier-Transform Infrared (FTIR) Spectroscopy

Infrared spectra were recorded using a Thermo Nicolet 380 FT-IR spectrometer (Thermo Scientific, Waltham, MA, USA) equipped with a Smart Orbit Diamond ATR system. Spectra were collected in absorbance mode over the range of 4000–400 cm^{-1}, with 68 scans per sample and a resolution of 8 cm^{-1}. Background spectra were collected prior to each sample measurement.

2.2.8. Mechanical Properties

Mechanical testing was performed on a TA.XT Plus Texture Analyzer (Stable Micro Systems, Godalming, UK) in accordance with ASTM D638. Specimens were held with 35 mm tensile grips, with an initial grip separation of 40 mm, and tested at a crosshead speed of 1 mm·min^{-1}.

2.2.9. Scanning Electron Microscopy (SEM)

A VEGA3 SBH scanning electron microscope (TESCAN, Brno, Czech Republic) was used to observe the microstructure of the recovered lignins. Samples were mounted on carbon tape and sputter-coated with a ca. 6 nm Au/Pd layer using an SPI Module Sputter Coater (90 s at 15 mA). Imaging was performed at accelerating voltages between 5 and 15 kV, with a working distance of 10 mm.

2.2.10. Thermogravimetric Analysis (TGA)

Thermal stability was assessed using a TG 209 F Tarsus thermogravimetric analyzer (Netzsch Instruments, Germany). Approximately 3 mg of sample was placed in an alumina crucible and heated from 25 °C to 500 °C at a rate of 10 °C·min^{-1} in a nitrogen atmosphere (flow rate: 50 mL min^{-1}).

2.2.11. Statistical Analysis

One-way ANOVA (α = 0.05) was used to evaluate statistical significance in water solubility, contact angle, DPPH radical scavenging activity, and mechanical properties. Data points with different letters are significantly different ($p < 0.05$) from each other.

3. Results and Discussion

3.1. PCL–Lignin Blends: Torque Rheometry and FTIR

The torque of the PCL-based blends was measured after incremental additions of lignin. The PCS–dealkalized lignin mixture was selected to illustrate the general behavior of the equilibrium torque as a function of lignin content (Figure 1). Similar profiles were obtained for all lignins. Up to 50 wt% lignin, the torque linearly increased, suggesting

higher material resistance, with an average increment of 0.029 ± 0.001 Nm (R^2 = 0.997) per wt% of lignin. However, from 60 to 100 wt%, the torque increased more sharply, with an increment of 0.042 ± 0.001 Nm (R^2 = 0.989) per wt% of lignin. This change suggests a critical concentration at ca. 50 wt%, beyond which a "solubility limit" is likely reached. At this point, the polymer blend may become less homogeneous, and the compatibility between PCL and lignin appears to decrease [30]. It is worth mentioning that the qualitative behavior of the other lignins is rather similar.

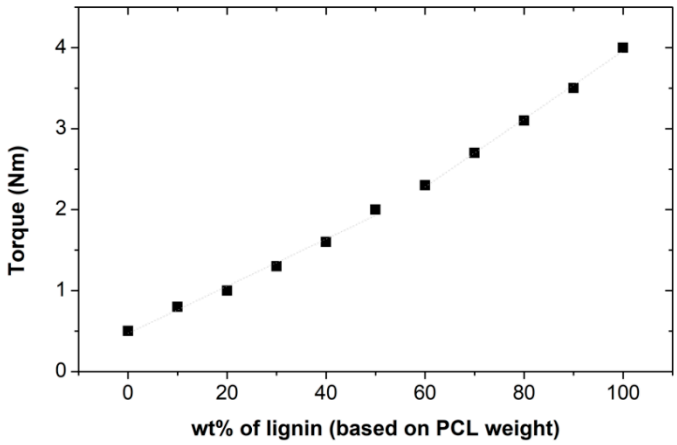

Figure 1. Torque rheometry dependence on dealkalized lignin addition. The dashed lines are linear fits of the data.

Figure 2 shows the IR spectra of PCL–lignin blends. The main characteristic bands of PCL are found at 2942 and 2865 cm^{-1} and assigned to the asymmetric and symmetric CH_2 stretching, respectively; 1720 cm^{-1} refers to carbonyl stretch; 1470 cm^{-1} corresponds to C-C bending; 1417, 1395, and 1365 cm^{-1} are assigned to the asymmetric CH_2 bending modes; 1293 cm^{-1} corresponds to the C-O and C-C stretching; 1238 cm^{-1} and 1162 cm^{-1} are attributed the asymmetric and symmetric C-O-C stretching, respectively; and the band at 1036 cm^{-1}, confirms the presence of C-O stretch of the ester group [31–33]. No significant differences were found between the spectra of neat PCL and any of the prepared PCL–lignin blends, meaning that, as seen via FTIR, lignin addition had no influence on the chemical nature of PCL.

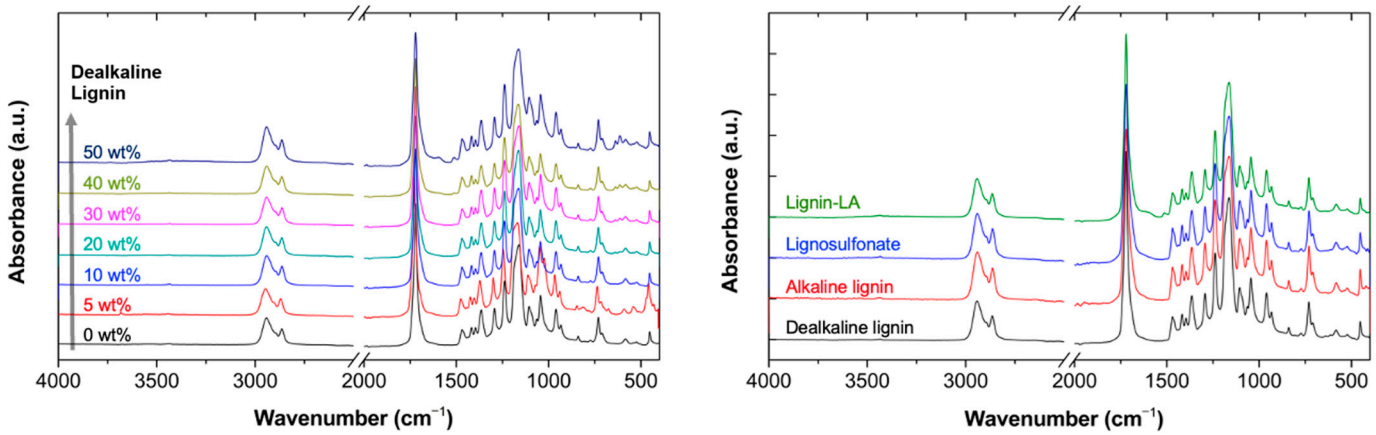

Figure 2. Normalized FTIR spectra of PCL with different concentrations of dealkalized lignin (**left**) and different types of lignin (20 wt%) (**right**).

3.2. Water Uptake and Water Solubility PLC–Lignin Blends

The water uptake of PCL–lignin mixtures was measured over time, as shown in Figure 3A,B. While neat PCL exhibited negligible water uptake, the equilibrium water

uptake increased with higher amounts of dealkalized lignin in the blend (Figure 3A) [34,35]. The maximum water uptake was reached after approximately 24 h. The water solubility of each blend was determined after 57 h of water immersion (Figure 3C), revealing a significant increase with increasing lignin content. Furthermore, the type of lignin also influenced both water uptake and solubility. Blends incorporating alkaline lignin and lignosulfonate displayed a rapid initial water uptake, followed by a slight decrease for alkaline lignin and a more pronounced reduction for lignosulfonate. This decrease is attributed to the higher solubility of these blends (Figure 3D), likely due to poor compatibility between PCL and lignosulfonate, leading to material loss and reduced water retention. Another possible explanation is the increased affinity of water for the lignosulfonate-containing matrix, resulting in elevated water activity—a phenomenon akin to a "salting-in-like" effect. This may trigger water release and subsequent matrix shrinkage as a mechanism to re-establish chemical potential equilibrium (REF). This is consistent with the observation that the PCL–lignosulfonate blend exhibited the highest water solubility (Figure 3D). In contrast, the lignin extracted using levulinic acid (lignin–LA) demonstrated greater compatibility with PCL. Composites containing lignin–LA exhibited the lowest water uptake (1% after one day) and lowest water solubility (0.6%) among all tested blends, highlighting the promising potential of using lignin–LA in PCL-based applications without the need for compatibilizing agents to enhance the miscibility and adhesion between PCL and lignin [31,36].

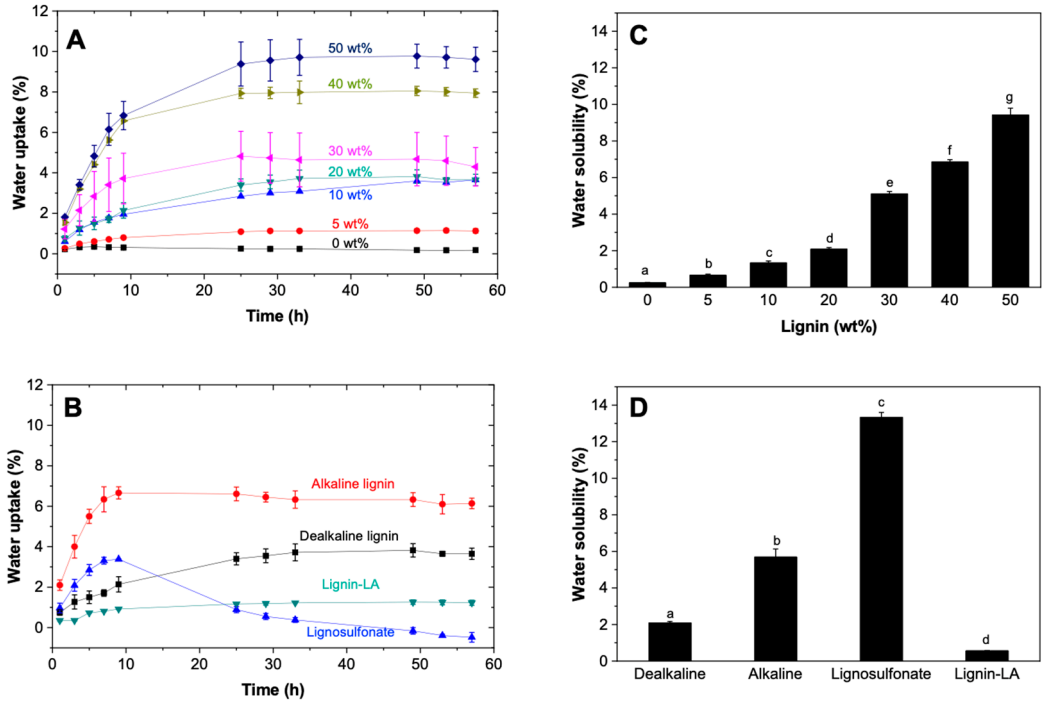

Figure 3. Water uptake (**A**,**B**) and water solubility (**C**,**D**) of PCL with different concentrations of dealkalized lignin (**A**,**C**) and different types of lignin (20 wt%) (**B**,**D**). Data points with different letters are significantly different ($p < 0.05$) from each other.

The water sorption mechanism was evaluated by fitting the linearized form of Equation (2) to the experimental kinetic data. The corresponding fitting parameters are summarized in Table 1. For blends with a low lignin content, water sorption follows a Fickian or pseudo-Fickian diffusion behavior through the material matrix. Fickian diffusion is characterized by a steady mass increase and an initial linear relationship between water uptake and time, followed by an asymptotic approach to equilibrium. This indicates that the kinetics of water sorption are primarily governed by the water activity gradient [37,38]. However, in systems containing more than 30 wt% of dealkalized lignin, the sorption

kinetics shift to a non-Fickian or anomalous regime (with values of the diffusional exponent n between 0.5 and 1). This behavior typically reflects the system's inability to rapidly reach equilibrium and occurs when the mobility of polymer chains is comparable to the diffusion rate [38,39]. This deviation is characterized by a prolonged mass increase during the later stages of sorption or a slower approach to the equilibrium plateau, which is indicative of a coupled diffusion–relaxation mechanism. Generally, such relaxation is associated with internal stresses that develop within the polymer matrix during swelling [38,40]. This transition in behavior becomes more evident as lignin content increases. Higher lignin concentrations result in greater water uptake and solubility, leading to increased mass loss and a marked deviation from Fickian-type diffusion. Additionally, the type of lignin significantly influenced the water diffusion behavior. When 20 wt% of dealkalized lignin—particularly lignin–LA—was added, the diffusion process remained predominantly Fickian ($n \leq 0.5$). In contrast, the addition of alkaline lignin induced a non-Fickian behavior ($n > 0.5$), aligning with the higher water solubility and lower apparent compatibility observed in the PCL/alkaline lignin blends.

Table 1. Fitting parameters of Equation (2) to experimental sorption of water from PCL–lignin blend membranes.

Type of Lignin	Lignin (wt%)	k/(s^{-n})	n (±s)	MST/(s)
Dealkaline	0	-	-	-
	5	4.99×10^{-3}	0.49 (±0.02)	16,200
	20	1.80×10^{-2}	0.46 (±0.03)	2130
	30	1.64×10^{-2}	0.53 (±0.01)	859
	40	7.56×10^{-3}	0.65 (±0.01)	719
	50	1.06×10^{-2}	0.63 (±0.01)	554
Alkaline	20	1.71×10^{-2}	n.d. *	n.d. *
Lignin-LA	20	8.48×10^{-3}	0.46 (±0.01)	11,200

* n.d. due to the speed of the sorption process.

Another relevant parameter in the analysis is the sorption rate constant, k. Since the dimensionality of k depends on the value of n, the direct comparison of k values across different composites is not meaningful. However, these values can be normalized using n through the so-called mean sorption time (MST) [41]. The MST allows for the comparison of swelling kinetics characterized by different sorption mechanisms and is defined as follows:

$$\mathrm{MST} = \left(\frac{\mathrm{n}}{\mathrm{n}+1}\right)\mathrm{k}^{-\mathrm{n}^{-1}} \tag{5}$$

where k and n have the same meaning as in Equation (2). A strong dependence of MST on the dealkalized lignin content in the composites was observed. Water sorption occurs more rapidly as the lignin content increases, thus suggesting that lignin enhances the water uptake rate. Furthermore, MST also depends on the type of lignin, aligning with the water solubility data, where the least soluble lignin, lignin–LA, exhibited the highest MST (in seconds) [42].

The analysis of the water uptake kinetics over the entire time range was further assessed by using first- and second-order kinetic equations, respectively, as follows:

$$\mathrm{m_{w,t}} = \mathrm{m_{w,eq}}\left(1 - \mathrm{e}^{-\mathrm{k,t}}\right) \tag{6}$$

$$\mathrm{m_{w,t}} = \frac{\mathrm{m_{w,eq}^2 k_2 t}}{1 + \mathrm{m_{w,eq} k_2 t}} \tag{7}$$

where k_1 and k_2 are the swelling (water uptake) rate constants [43].

The fitting of Equations (6) and (7) to the experimental data indicated that, in general, the swelling kinetics follow a first-order kinetic mechanism (Figure S1). The goodness of the fit was evaluated using determination coefficients (R^2) and Akaike's information criteria (*AIC*) [42,44], which is calculated as follows:

$$\mathrm{AIC} = \mathrm{N}\log\left(\frac{\mathrm{s}^2}{\mathrm{N}}\right) + 2\mathrm{K} + \frac{2\mathrm{K}(\mathrm{K}+1)}{\mathrm{N}-\mathrm{K}-1} \quad (8)$$

where s^2 is the residual sum of squares, N is the number of experimental data points, and K is the number of model-independent fitting parameters. Equation (8) is valid for $N/K < 40$.

The fitting results indeed confirm that the water uptake kinetics generally follow a first-order kinetic mechanism. This is consistent with the behavior observed at short time scales (Table 1), suggesting that water–water interactions dominate over water–polymer interactions. This is further supported by the fact that the rate constant, k_1, remains largely unaffected by the lignin content in the PCL composites (Figure S2b), with an average value of 0.16 ($\pm$0.02) h^{-1}. Nevertheless, increasing lignin content clearly leads to an increase in the maximum water uptake (Figure S2a).

3.3. Surface Properties of PCL–Lignin Blends: Hydrophilicity and Antioxidant Capacity

Neat PCL exhibits a moderately hydrophilic surface, with a water contact angle of 77 $\pm$ 2° (Figure 4). Incorporating dealkaline lignin into the composite significantly enhances surface hydrophobicity: as the lignin content increases from 5 to 20 wt%, the contact angle rises, exceeding 90° for lignin loadings above 10 wt% (reaching 92 $\pm$ 1°). Maximum hydrophobicity is achieved with 20 and 30 wt% dealkalized lignin, yielding contact angles of 101 $\pm$ 3° and 103 $\pm$ 2°, respectively. When lignin–LA is used, the results are comparable to those observed with dealkalized lignin. In contrast, the addition of lignosulfonate or alkaline lignin leads to a marked decrease in contact angle, likely due to their greater hydrophilicity and higher water solubility [45,46].

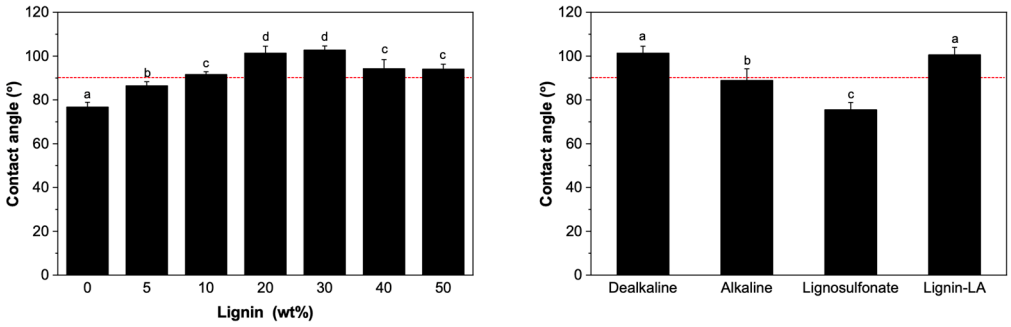

Figure 4. Water contact angle of PCL composites with varying concentrations of dealkalized lignin (**left**) and with different types of lignin at 20 wt% (**right**). The red line indicates the threshold for hydrophobicity. Data points labeled with different letters are significantly different from each other ($p < 0.05$).

Regarding bioactivity, a modest antioxidant activity was observed for neat PCL, displaying a DPPH radical scavenging activity (RSA) of 8 $\pm$ 1% (Figure 5). Remarkably, the incorporation of lignin significantly enhanced this effect. The addition of just 5 wt% dealkaline lignin enhanced the RSA to 91.7 $\pm$ 0.01%, with a slight further increase at higher lignin contents, reaching 95.1 $\pm$ 0.3% at 50 wt%.

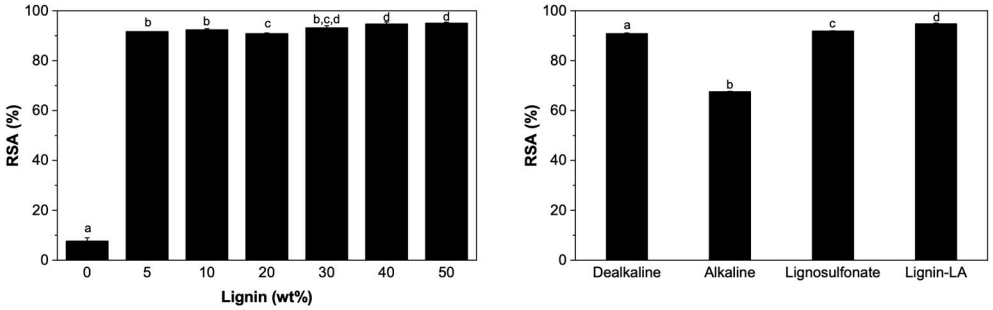

Figure 5. DPPH radical scavenging activity (RSA) of PCL composites with varying concentrations of dealkalized lignin (**left**) and different types of lignin at 20 wt% (**right**). Data points labeled with different letters are significantly different from each other ($p < 0.05$).

When comparing lignin types, alkaline lignin resulted in the lowest RSA (67.6 ± 0.1%), whereas blends containing lignin–LA showed the highest antioxidant activity (94.8 ± 0.3%). This trend is consistent with the literature, in which lignins with lower molecular weights—typically enriched in phenolic hydroxyl and carboxyl groups—exhibit superior antioxidant performance. In particular, lignin–LA, with an average molecular weight around 3 kDa, outperformed both lignosulfonate (up to 150 kDa) and alkali lignin (generally above 10 kDa), reinforcing the key role of lignin structure in determining antioxidant efficacy.

Subtle antioxidant activity was detected for neat PCL, with a DPPH radical scavenging activity (RSA) of 8 ± 1% (Figure 5). Remarkably, the incorporation of lignin dramatically enhanced this effect: just 5 wt% dealkaline lignin boosted the RSA to 91.7 ± 0.01%, with a slight further increase observed at higher lignin loadings (up to 95.1 ± 0.3% at 50 wt%). When comparing different lignin types, alkaline lignin yielded the lowest RSA (67.6 ± 0.1%), while PCL–lignin–LA composites exhibited the highest antioxidant activity (94.8 ± 0.3%). This trend aligns with literature reports, as lower-molecular weight lignins, which are typically richer in phenolic hydroxyl and carboxyl groups, demonstrate superior antioxidant capacity [47,48]. Notably, lignin–LA, with an average molecular weight near 3 kDa, outperforms lignosulfonate (up to 150 kDa) and alkali lignin (typically above 10 kDa), supporting the strong relationship between lignin structure and antioxidant performance [25,49,50].

3.4. Mechanical and Morphological Features

In general, the addition of lignin significantly reduced both the tensile strength and elongation at break of neat PCL (Figure 6d). Neat PCL exhibited a tensile strength of 21.0 ± 0.7 MPa, which progressively decreased with increasing dealkalized lignin content, reaching 9 ± 1 MPa in systems containing 50 wt% lignin. A similar trend was observed for elongation at break, with the most pronounced reduction occurring up to 20 wt% lignin, after which the decline continued at a slower rate.

This reduction in mechanical performance can be attributed to the aggregation of lignin molecules at higher concentrations, which restricts polymer chain mobility and increases rigidity while diminishing the material's ability to absorb stress. As the lignin content increases, the incompatibility between PCL and lignin becomes more pronounced, resulting in poor interfacial adhesion, greater phase separation, and consequently, reduced tensile strength [51]. This structural incompatibility is further supported by the SEM micrographs obtained for cross-sections of neat PCL and PCL–lignin blends (Figure 6a–c), which reveal the formation of an increasingly less homogeneous and rougher morphology as the lignin content increases.

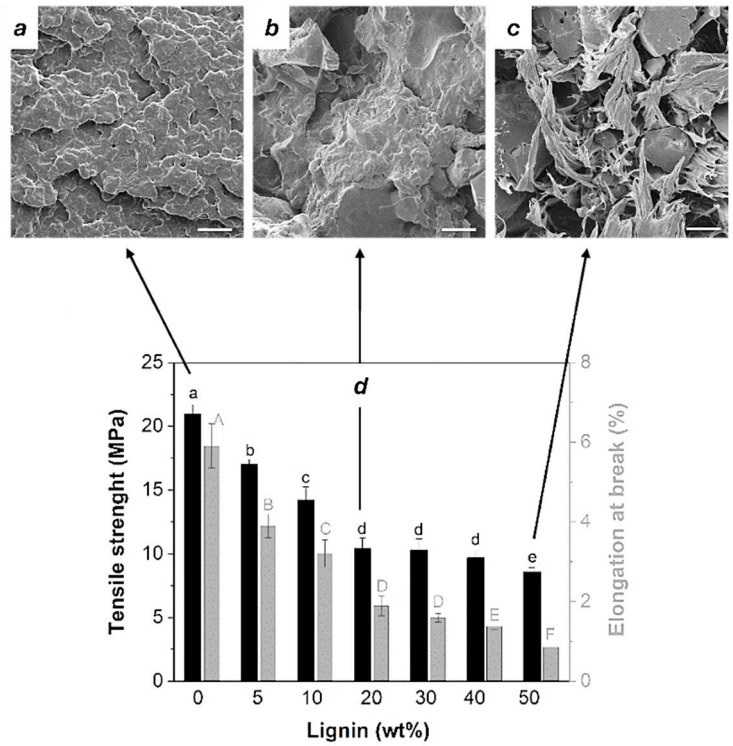

Figure 6. SEM micrographs of cross-sections of neat PCL (scale bars = 20 µm) (**a**) and PCL–lignin composites containing 20 wt% (**b**) and 50 wt% (**c**) dealkalized lignin, showing increased surface roughness and heterogeneity with lignin content. (**d**) Mechanical properties of PCL composites with varying concentrations of dealkalized lignin, highlighting the impact on tensile strength (black bars) and elongation at break (grey bars). Data points labeled with different letters are significantly different from each other ($p < 0.05$).

Tensile strength and elongation at break are also observed to be influenced by the type of lignin used in the blend. Interestingly, the addition of 20 wt% alkali lignin or lignosulfonate resulted in the least impact on mechanical properties among all tested lignins. Although the incorporation of 20 wt% dealkaline lignin and lignin–LA yielded composites with statistically similar tensile strength and elongation at break, their cross-sectional morphologies differed significantly (Figure 7). Notably, the system containing 20 wt% lignin–LA exhibited a cross-section resembling that of the 50 wt% dealkalized lignin blends (Figure 6c), despite maintaining mechanical properties similar to those with lower lignin contents. These differences among the various lignin types may be attributed to disparities in molecular weight (Table 2) and the number of functional groups, as lignin–LA and dealkalized lignin generally possess lower molecular weights than lignosulfonate and alkaline lignin [25,52]. The extracted lignin (lignin–LA) was found to be notably rich in carbonyl groups compared to its commercial counterparts. The latter two also presented with compact structures with a high number of phenyl-OH groups and aliphatic OH groups between 1 and 1.7 $mmolg^{-1}$, as lignosulfonate also contains sulfonate groups [53]. In contrast, previously reported data showed that condensed OH structures and acidic groups are present in lignin–LA. The obtained lignin–LA ^{31}P NMR data showed the presence of guaiacyl units, C5-substituted condensed guaiacyl, and almost no aliphatic OH groups, while enriched C-O groups possibly originated from the partial OH-esterification with LA. The phenolic hydroxyl content was estimated as 0.56 mmol g^{-1} [26].

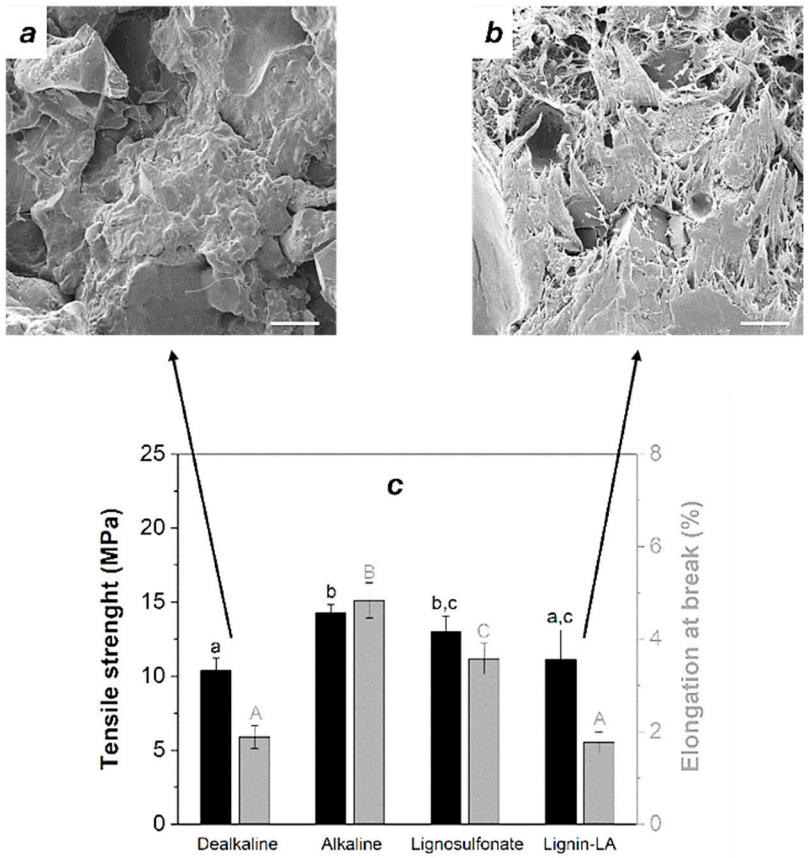

Figure 7. SEM micrographs (top) of cross sections of PCL–lignin composites (scale bars = 20 µm) containing 20 wt% dealkalized lignin (**a**) and lignin–LA (**b**). Mechanical properties (tensile strength (black bars) and elongation at break (grey bars)) of PCL with different lignin types (**c**). Data points labeled with different letters are significantly different from each other ($p < 0.05$).

Table 2. Lignins used in this work and their respective molecular weights (M_w).

Type of Lignin	M_W (Da)
Dealkaline	10,263
Alkali	6024
Lignosulfonate	4881
Lignin-LA	3697

3.5. Thermal Stability of PCL–Lignin Blends

The thermal behavior of the PCL–lignin blends was evaluated using thermogravimetric analysis (TGA), revealing significant differences primarily associated with the type of lignin used (Figure 8 and Table S1). The incorporation of increasing amounts of dealkalized lignin significantly reduced the onset of weight loss (Figure 8a,b) while simultaneously increasing the residual mass at 500 °C, reaching up to 27.2% in composites containing 50 wt% dealkalized lignin (Table S1). This finding suggests that the addition of lignin affects the stability of the polymer matrix, likely promoting water solubility and altering the decomposition behavior.

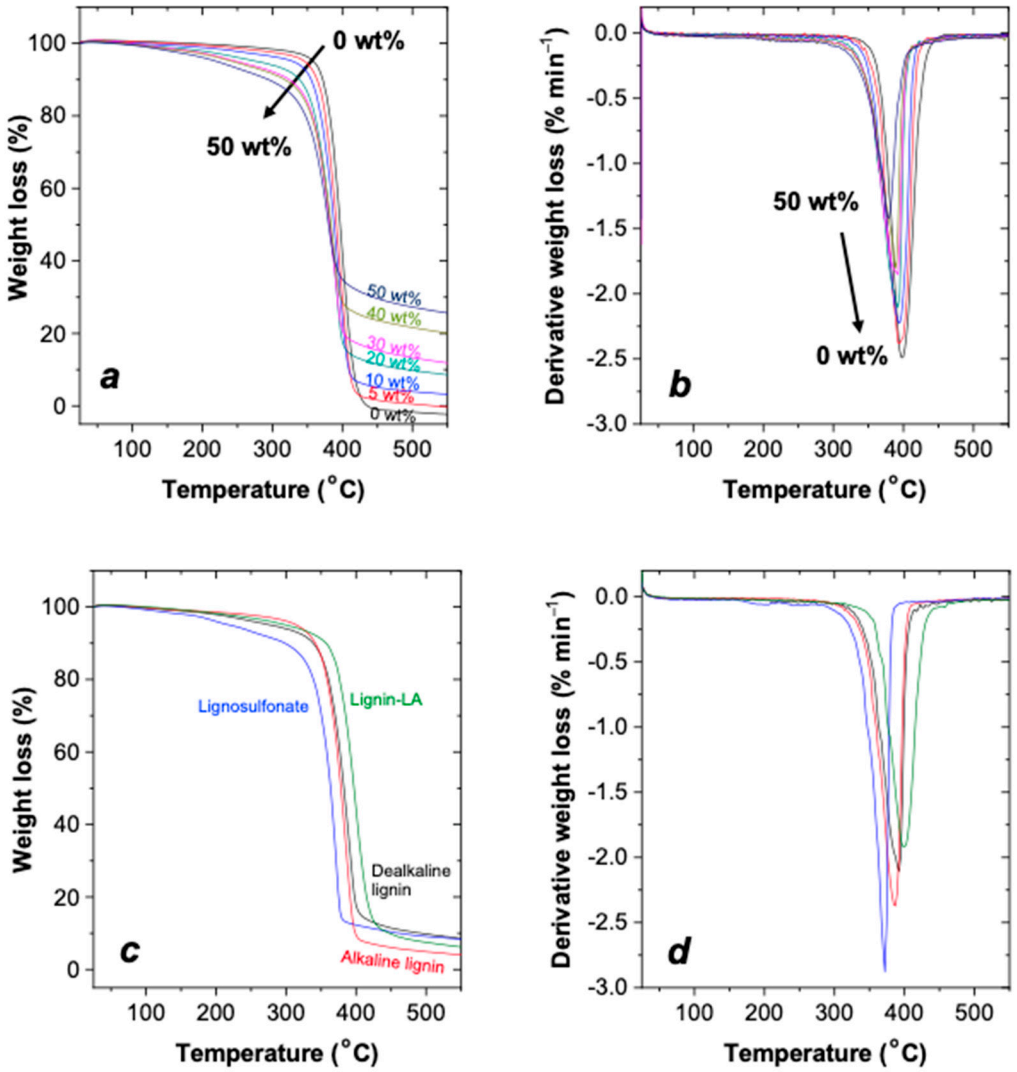

Figure 8. Thermograms (**a**,**c**) and corresponding derivative thermogravimetric curves (**b**,**d**) for PCL–lignin blends. Panels (**a**,**b**) show the effect of increasing concentrations of dealkalized lignin, while panels (**c**,**d**) compare composites containing 20 wt% of each type of lignin.

When comparing systems with 20 wt% of each lignin, dealkalized lignin produced the highest residue (9.8%), followed by lignosulfonate (9.1%), lignin–LA (7.5%), and alkaline lignin (4.9%). These residues are consistent with the known decomposition patterns and impurity profiles of different lignins [54,55].

Interestingly, despite the overall decrease in thermal stability with lignin incorporation, both the temperature at 50% weight loss and the maximum decomposition temperature were largely preserved in composites containing lignin–LA. The thermal degradation behavior of these composites remained closer to that of neat PCL, suggesting improved compatibility between lignin–LA and the polymer matrix [56,57].

4. Conclusions

This study successfully incorporated various amounts and types of lignin into a PCL matrix, revealing significant differences in performance depending on lignin type and concentration. Remarkably, the addition of up to 50 wt% dealkalized lignin did not alter the chemical nature of PCL but significantly enhanced water uptake and solubility with increasing lignin content. While lignin–LA blends showed the lowest water uptake improvement among the lignins tested, they exhibited the lowest water solubility, thus

suggesting a higher compatibility between lignin–LA and the PCL matrix. Although it compromised tensile strength and elongation at break, the addition of lignin proved to increase other properties of PCL. Blends composed of lignin–LA showed morphological features at lower concentrations comparable to blends with higher amounts of dealkalized lignin, while still preserving mechanical properties and thermal stability.

Overall, composite hydrophobicity increased with lignin incorporation, except in the case of lignosulfonate, likely due to its intrinsic water solubility. Importantly, all lignin-containing composites demonstrated pronounced antioxidant activity, a feature that is absent in neat PCL. This finding positions lignin as a promising candidate for use in active packaging systems or other applications in which oxidative stability is critical.

This work also highlights the potential of using green solvents such as levulinic acid to enhance lignin's value, thereby opening promising routes for the development of biodegradable, multifunctional blends and composites where antioxidant protection, water resistance, and sustainability are prioritized over mechanical reinforcement.

Supplementary Materials: The following supporting information can be downloaded at https://www.mdpi.com/article/10.3390/jcs9070366/s1: Figure S1: Representative water uptake kinetics of PCL-based blends containing different amounts of lignin; Figure S2: Fitting parameters, $m_{w,eq}$ and k_1, obtained from Equation (3) applied to experimental water uptake data for various PCL–lignin blends, Table S1: Thermal properties of PCL–lignin blends.

Author Contributions: Conceptualization, E.M. and H.D.; methodology, E.M. and F.E.A.; validation, A.J.M.V., A.R. and B.M.; formal analysis, E.M.; investigation, E.M.; data curation, A.J.M.V.; writing—original draft preparation, E.M. and H.D.; writing—review and editing, E.M., H.D., F.E.A., A.J.M.V. and B.M.; visualization, F.E.A. and B.M.; supervision, A.J.M.V., A.R. and B.M. All authors have read and agreed to the published version of the manuscript.

Funding: This work was supported by funding from the Portuguese Foundation for Science and Technology (FCT) through the individual research contract CEECIND/01014/2018 (DOI: https://doi.org/10.54499/CEECIND/01014/2018/CP1540/CT0002 accessed on 9 July 2025). This research was financed by National Funds through FCT-Foundation for Science and Technology under the Projects MED UIDB/05183 (doi:10.54499/UIDB/05183 and doi:10.54499/UIDP/05183) and CHANGE (doi:10.54499/LA/P/0121/2020). CQC is supported by the FCT through the projects UID/QUI/00313/2020 and COMPETE. H.D. We would also like to thank Fundação la Caixa and the FCT for the financial support through the project "Plantas aromáticas do Alentejo, probióticos e farinha de bolota no desenvolvimento de pão funcional" (PD23-0025).

Data Availability Statement: Dataset available on request from the authors.

Conflicts of Interest: The authors declare no conflicts of interest.

References

1. Labet, M.; Thielemans, W. Synthesis of Polycaprolactone: A Review. *Chem. Soc. Rev.* **2009**, *38*, 3484–3504. [CrossRef]
2. Okada, M. Chemical Syntheses of Biodegradable Polymers. *Prog. Polym. Sci.* **2002**, *27*, 87–133. [CrossRef]
3. Nawaz, A.; Hasan, F.; Shah, A.A. Degradation of Poly(ε-Caprolactone) (PCL) by a Newly Isolated *Brevundimonas* Sp. Strain MRL-AN1 from Soil. *FEMS Microbiol. Lett.* **2015**, *362*, 1–7. [CrossRef] [PubMed]
4. Nair, L.S.; Laurencin, C.T. Biodegradable Polymers as Biomaterials. *Prog. Polym. Sci.* **2007**, *32*, 762–798. [CrossRef]
5. Hutmacher, D.W.; Schantz, T.; Zein, I.; Ng, K.W.; Teoh, S.H.; Tan, K.C. Mechanical Properties and Cell Cultural Response of Polycaprolactone Scaffolds Designed and Fabricated via Fused Deposition Modeling. *J. Biomed. Mater. Res.* **2001**, *55*, 203–216. [CrossRef]
6. Joy, A.; Unnikrishnan, G.; Megha, M.; Haris, M.; Thomas, J.; Kolanthai, E.; Muthuswamy, S. Polycaprolactone/Graphene Oxide–Silver Nanocomposite: A Multifunctional Agent for Biomedical Applications. *J. Inorg. Organomet. Polym.* **2022**, *32*, 912–930. [CrossRef]

7. Shi, C.; Zhou, A.; Fang, D.; Lu, T.; Wang, J.; Song, Y.; Lyu, L.; Wu, W.; Huang, C.; Li, W. Oregano Essential Oil/β-Cyclodextrin Inclusion Compound Polylactic Acid/Polycaprolactone Electrospun Nanofibers for Active Food Packaging. *Chem. Eng. J.* **2022**, *445*, 136746. [CrossRef]
8. Bartnikowski, M.; Dargaville, T.R.; Ivanovski, S.; Hutmacher, D.W. Degradation Mechanisms of Polycaprolactone in the Context of Chemistry, Geometry and Environment. *Prog. Polym. Sci.* **2019**, *96*, 1–20. [CrossRef]
9. Woodruff, M.A.; Hutmacher, D.W. The Return of a Forgotten Polymer—Polycaprolactone in the 21st Century. *Prog. Polym. Sci.* **2010**, *35*, 1217–1256. [CrossRef]
10. Melro, E.; Filipe, A.; Sousa, D.; Medronho, B.; Romano, A. Revisiting Lignin: A Tour through Its Structural Features, Characterization Methods and Applications. *New J. Chem.* **2021**, *45*, 6986–7013. [CrossRef]
11. Cao, X.; Huang, J.; He, Y.; Hu, C.; Zhang, Q.; Yin, X.; Wu, W.; Li, R.K.Y. Biodegradable and Renewable UV-Shielding Polylactide Composites Containing Hierarchical Structured POSS Functionalized Lignin. *Int. J. Biol. Macromol.* **2021**, *188*, 323–332. [CrossRef] [PubMed]
12. Park, S.Y.; Kim, J.-Y.; Youn, H.J.; Choi, J.W. Utilization of Lignin Fractions in UV Resistant Lignin-PLA Biocomposites via Lignin-Lactide Grafting. *Int. J. Biol. Macromol.* **2019**, *138*, 1029–1034. [CrossRef] [PubMed]
13. Kazzaz, A.E.; Feizi, Z.H.; Fatehi, P. Grafting Strategies for Hydroxy Groups of Lignin for Producing Materials. *Green Chem.* **2019**, *21*, 5714–5752. [CrossRef]
14. Abdollahi, M.; Bairami Habashi, R.; Mohsenpour, M. Poly(ε-Caprolactone) Chains Grafted from Lignin, Hydroxymethylated Lignin and Silica/Lignin Hybrid Macroinitiators: Synthesis and Characterization of Lignin- Based Thermoplastic Copolymers. *Ind. Crops Prod.* **2019**, *130*, 547–557. [CrossRef]
15. Beniwal, P.; Guliani, D.; Toor, A.P. Influence of Functionalised Lignin on Strength and Antioxidant Properties of Polylactic Acid Films. *J. Polym. Res.* **2024**, *31*, 68. [CrossRef]
16. Zhang, N.; Zhao, M.; Liu, G.; Wang, J.; Chen, Y.; Zhang, Z. Alkylated Lignin with Graft Copolymerization for Enhancing Toughness of PLA. *J. Mater. Sci.* **2022**, *57*, 8687–8700. [CrossRef]
17. Wang, J.; Tian, L.; Luo, B.; Ramakrishna, S.; Kai, D.; Loh, X.J.; Yang, I.H.; Deen, G.R.; Mo, X. Engineering PCL/Lignin Nanofibers as an Antioxidant Scaffold for the Growth of Neuron and Schwann Cell. *Colloids Surf. B Biointerfaces* **2018**, *169*, 356–365. [CrossRef]
18. Parit, M.; Jiang, Z. Towards Lignin Derived Thermoplastic Polymers. *Int. J. Biol. Macromol.* **2020**, *165*, 3180–3197. [CrossRef]
19. Adams, B.; Abdelwahab, M.; Misra, M.; Mohanty, A.K. Injection-Molded Bioblends from Lignin and Biodegradable Polymers: Processing and Performance Evaluation. *J. Polym. Environ.* **2018**, *26*, 2360–2373. [CrossRef]
20. Teramoto, Y.; Lee, S.-H.; Endo, T. Phase Structure and Mechanical Property of Blends of Organosolv Lignin Alkyl Esters with Poly(ε-Caprolactone). *Polym. J.* **2009**, *41*, 219–227. [CrossRef]
21. Teramoto, Y.; Lee, S.-H.; Endo, T.; Nishio, Y. Scale of Homogeneous Mixing in Miscible Blends of Organosolv Lignin Esters with Poly(ε-Caprolactone). *J. Wood Chem. Technol.* **2010**, *30*, 330–347. [CrossRef]
22. Nitz, H.; Semke, H.; Landers, R.; Mülhaupt, R. Reactive Extrusion of Polycaprolactone Compounds Containing Wood Flour and Lignin. *J. Appl. Polym. Sci.* **2001**, *81*, 1972–1984. [CrossRef]
23. Pucciariello, R.; D'Auria, M.; Villani, V.; Giammarino, G.; Gorrasi, G.; Shulga, G. Lignin/Poly(ε-Caprolactone) Blends with Tuneable Mechanical Properties Prepared by High Energy Ball-Milling. *J. Polym. Environ.* **2010**, *18*, 326–334. [CrossRef]
24. Pucciariello, R.; Villani, V.; Bonini, C.; D'Auria, M.; Vetere, T. Physical Properties of Straw Lignin-Based Polymer Blends. *Polymer* **2004**, *45*, 4159–4169. [CrossRef]
25. Melro, E.; Riddell, A.; Bernin, D.; da Costa, A.M.R.; Valente, A.J.M.; Antunes, F.E.; Romano, A.; Norgren, M.; Medronho, B. Levulinic Acid-Based "Green" Solvents for Lignocellulose Fractionation: On the Superior Extraction Yield and Selectivity toward Lignin. *Biomacromolecules* **2023**, *24*, 3094–3104. [CrossRef]
26. Melro, E.; Duarte, H.; Antunes, F.E.; Valente, A.J.M.; Romano, A.; Norgren, M.; Medronho, B. Engineering Novel Phenolic Foams with Lignin Extracted from Pine Wood Residues via a New Levulinic-Acid Assisted Process. *Int. J. Biol. Macromol.* **2023**, *248*, 125947. [CrossRef]
27. *ASTM D570-98*; Standard Test Method for Water Absorption of Plastics. ASTM International: New York, NY, USA, 1998. [CrossRef]
28. Crank, J. *The Mathematics of Diffusion*, 2nd ed.; reprint; Clarendon Press: Oxford, UK, 1976; ISBN 978-0-19-853344-3.
29. Alzagameem, A.; Klein, S.E.; Bergs, M.; Do, X.T.; Korte, I.; Dohlen, S.; Hüwe, C.; Kreyenschmidt, J.; Kamm, B.; Larkins, M.; et al. Antimicrobial Activity of Lignin and Lignin-Derived Cellulose and Chitosan Composites against Selected Pathogenic and Spoilage Microorganisms. *Polymers* **2019**, *11*, 670. [CrossRef]
30. Melro, E.; Duarte, H.; Eivazi, A.; Costa, C.; Faleiro, M.L.; da Costa, A.M.R.; Antunes, F.E.; Valente, A.J.M.; Romano, A.; Norgren, M.; et al. Poly(Butylene Succinate)-Based Composites with Technical and Extracted Lignins from Wood Residues. *ACS Appl. Polym. Mater.* **2024**, *6*, 1169–1181. [CrossRef]

31. Xie, D.; Pu, Y.; Meng, X.; Bryant, N.D.; Zhang, K.; Wang, W.; Ragauskas, A.J.; Li, M. Effect of the Lignin Structure on the Physicochemical Properties of Lignin-Grafted-Poly(ε-Caprolactone) and Its Application for Water/Oil Separation. *ACS Sustain. Chem. Eng.* **2022**, *10*, 16882–16895. [CrossRef]
32. Palacios Hinestroza, H.; Urena-Saborio, H.; Zurita, F.; Guerrero de León, A.A.; Sundaram, G.; Sulbarán-Rangel, B. Nanocellulose and Polycaprolactone Nanospun Composite Membranes and Their Potential for the Removal of Pollutants from Water. *Molecules* **2020**, *25*, 683. [CrossRef]
33. Janarthanan, G.; Kim, I.G.; Chung, E.-J.; Noh, I. Comparative Studies on Thin Polycaprolactone-Tricalcium Phosphate Composite Scaffolds and Its Interaction with Mesenchymal Stem Cells. *Biomater. Res.* **2019**, *23*, 1. [CrossRef]
34. Kim, B.; Lee, J.; Jang, S.; Park, J.; Choi, J.; Lee, S.; Jung, J.; Park, J. Exploring the Effect of the Polyol Structure and the Incorporation of Lignin on the Properties of Bio-Based Polyurethane. *Polymers* **2025**, *17*, 604. [CrossRef] [PubMed]
35. Haider, M.K.; Kharaghani, D.; Sun, L.; Ullah, S.; Sarwar, M.N.; Ullah, A.; Khatri, M.; Yoshiko, Y.; Gopiraman, M.; Kim, I.S. Synthesized Bioactive Lignin Nanoparticles/Polycaprolactone Nanofibers: A Novel Nanobiocomposite for Bone Tissue Engineering. *Biomater. Adv.* **2023**, *144*, 213203. [CrossRef] [PubMed]
36. Trinh, B.M.; Gupta, A.; Owen, P.; David, D.; Yim, E.; Mekonnen, T.H. Compostable Lignin Grafted Poly(ε-Caprolactone) Polyurethane Biomedical Materials: Shape Memory, Foaming Capabilities, and Biocompatibility. *Chem. Eng. J.* **2024**, *485*, 149845. [CrossRef]
37. Karimi, M. Diffusion in Polymer Solids and Solutions. In *Mass Transfer in Chemical Engineering Processes*; IntechOpen: London, UK, 2011; ISBN 978-953-307-619-5.
38. Starkova, O.; Aiello, M.A.; Aniskevich, A. Long-Term Moisture Diffusion in Vinylester Resin and CFRP Rebars: A 20-Year Case Study. *Compos. Sci. Technol.* **2023**, *242*, 110167. [CrossRef]
39. Hassanpour, B.; Karbhari, V.M. Characteristics and Models of Moisture Uptake in Fiber-Reinforced Composites: A Topical Review. *Polymers* **2024**, *16*, 2265. [CrossRef]
40. Starkova, O.; Chandrasekaran, S.; Schnoor, T.; Sevcenko, J.; Schulte, K. Anomalous Water Diffusion in Epoxy/Carbon Nanoparticle Composites. *Polym. Degrad. Stab.* **2019**, *164*, 127–135. [CrossRef]
41. Sriamornsak, P.; Sungthongjeeh, S. Modification of Theophylline Release with Alginate Gel Formed in Hard Capsules. *AAPS PharmSciTech* **2007**, *8*, 51. [CrossRef] [PubMed]
42. Ferreira, A.C.S.; Aguado, R.; Carta, A.M.M.S.; Bértolo, R.; Murtinho, D.; Valente, A.J.M. Influence of DNA as Additive for Market Pulp on Tissue Paper. *Nord. Pulp Pap. Res. J.* **2022**, *37*, 489–496. [CrossRef]
43. Quintana, J.R.; Valderruten, N.E.; Katime, I. Synthesis and Swelling Kinetics of Poly(Dimethylaminoethyl Acrylate Methyl Chloride Quaternary-Co-Itaconic Acid) Hydrogels. *Langmuir* **1999**, *15*, 4728–4730. [CrossRef]
44. Cova, F.; Murtinho, D.; Pais, A.A.C.C.; Valente, A.J.M.; Utzeri, G. Insights on Macro- and Microscopic Interactions between Confidor and Cyclodextrin-Based Nanosponges. *Chem. Eng. J.* **2023**, *455*, 140882.
45. Dutta, K.; Saikia, A.; Singh, A. Transforming Lignin into Polymer Film with Improved Physiochemical Properties by Modification with Itaconic Acid and Grafting with Polycaprolactone. *Int. J. Biol. Macromol.* **2025**, *305*, 141226. [CrossRef] [PubMed]
46. Liu, X.; Zong, E.; Jiang, J.; Fu, S.; Wang, J.; Xu, B.; Li, W.; Lin, X.; Xu, Y.; Wang, C.; et al. Preparation and Characterization of Lignin-Graft-Poly (-Caprolactone) Copolymers Based on Lignocellulosic Butanol Residue. *Int. J. Biol. Macromol.* **2015**, *81*, 521–529. [CrossRef] [PubMed]
47. Guiao, K.S.; Tzoganakis, C.; Mekonnen, T.H. Green Mechano-Chemical Processing of Lignocellulosic Biomass for Lignin Recovery. *Chemosphere* **2022**, *293*, 133647. [CrossRef] [PubMed]
48. Lu, X.; Gu, X.; Shi, Y. A Review on Lignin Antioxidants: Their Sources, Isolations, Antioxidant Activities and Various Applications. *Int. J. Biol. Macromol.* **2022**, *210*, 716–741. [CrossRef]
49. Guo, D.; Wu, S.; Lyu, G.; Guo, H. Effect of Molecular Weight on the Pyrolysis Characteristics of Alkali Lignin. *Fuel* **2017**, *193*, 45–53. [CrossRef]
50. Aro, T.; Fatehi, P. Production and Application of Lignosulfonates and Sulfonated Lignin. *ChemSusChem* **2017**, *10*, 1861–1877. [CrossRef]
51. Jiang, B.; Jiao, H.; Guo, X.; Chen, G.; Guo, J.; Wu, W.; Jin, Y.; Cao, G.; Liang, Z. Lignin-Based Materials for Additive Manufacturing: Chemistry, Processing, Structures, Properties, and Applications. *Adv. Sci.* **2023**, *10*, 2206055. [CrossRef]
52. Tian, J.; Yang, Y.; Song, J. Grafting Polycaprolactone onto Alkaline Lignin for Improved Compatibility and Processability. *Int. J. Biol. Macromol.* **2019**, *141*, 919–926. [CrossRef]
53. Taher, M.A.; Wang, X.; Faridul Hasan, K.M.; Miah, M.R.; Zhu, J.; Chen, J. Lignin Modification for Enhanced Performance of Polymer Composites. *ACS Appl. Bio. Mater.* **2023**, *6*, 5169–5192. [CrossRef]
54. Huang, X.; Yin, H.; Zhang, H.; Mei, N.; Mu, L. Pyrolysis Characteristics, Gas Products, Volatiles, and Thermo–Kinetics of Industrial Lignin via TG/DTG–FTIR/MS and in–Situ Py–PI–TOF/MS. *Energy* **2022**, *259*, 125062. [CrossRef]
55. Mousavioun, P.; Doherty, W.O.S. Chemical and Thermal Properties of Fractionated Bagasse Soda Lignin. *Ind. Crops Prod.* **2010**, *31*, 52–58. [CrossRef]

56. Hatakeyama, T.; Yamashita, S.; Hatakeyama, H. Thermal Properties of Lignin-Based Polycaprolactones. *J. Therm. Anal. Calorim.* **2021**, *143*, 203–211. [CrossRef]
57. Laurichesse, S.; Avérous, L. Synthesis, Thermal Properties, Rheological and Mechanical Behaviors of Lignins-*Grafted*-Poly(ε-Caprolactone). *Polymer* **2013**, *54*, 3882–3890. [CrossRef]